Science Advances
AAAS

advances.sciencemag.org/cgi/content/full/6/8/eaay8676/DC1

Supplementary Materials for

Transient invaders can induce shifts between alternative stable states of microbial communities

Daniel R. Amor*, Christoph Ratzke, Jeff Gore*

*Corresponding author. Email: gore@mit.edu (J.G.); damor@mit.edu (D.A.)

Published 19 February 2020, *Sci. Adv.* **6**, eaay8676 (2020)
DOI: 10.1126/sciadv.aay8676

This PDF file includes:

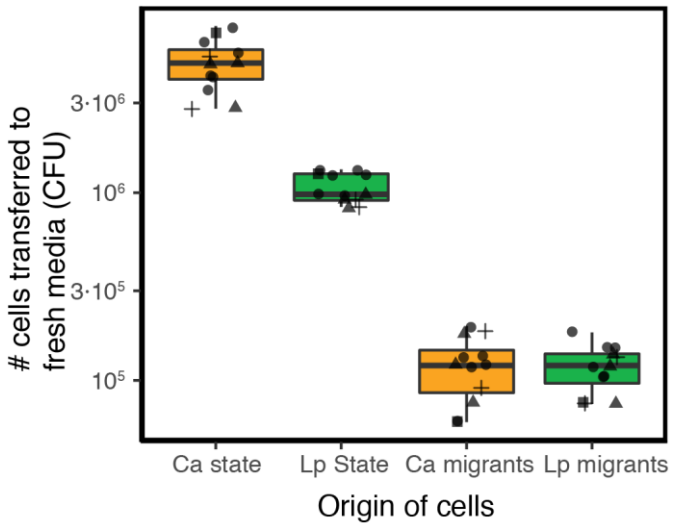

Fig. S1. Number of cells transferred to fresh media during daily dilution and migration steps. Box plot for the number of cells transferred from the *Ca* stable state, *Lp* stable state, or inoculated as *Ca* migrants and *Lp* migrants, respectively from left to right. Different symbol shapes stand for data from independent experiments, data points with the same shape correspond to technical replicates. The two data sets on the left also indicate that the *Ca* and the *Lp* stable states had different saturation densities (which correspond to 30x the average number of cells indicated in this panel), in agreement with the different saturation densities observed in the first and last data points in Figs. 1D, S3E, S3F and S4. The applied migration rate introduces $(1.2\pm0.1)\cdot10^5$ cells/day of each species. For this migration rate, *Ca* cells migrating into the *Lp* stable state constitute up to 10% of the total number of cells transferred at the beginning of each cycle, and up to 1% for the case of *Lp* cells migrating into the *Ca* stable state.

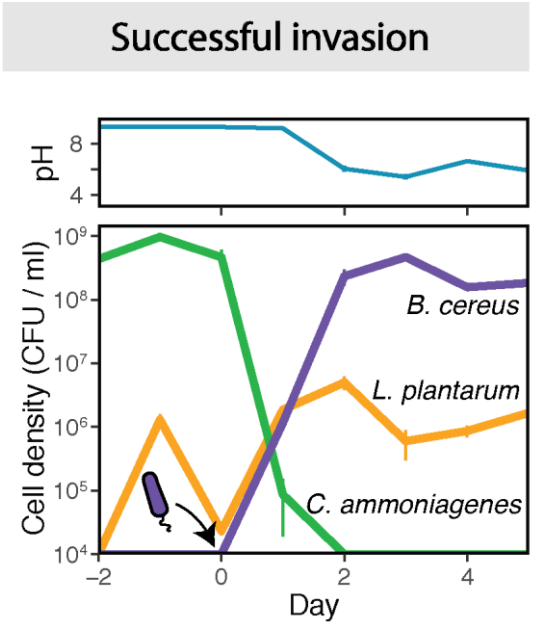

Fig. S2. Successful invasion by *Bc*. Applying daily dilution cycles including migration (Main Text), we initiated cocultures at a 5:95 ratio of *Lp* to *Ca* cells, allowing the first 3 cycles for the system to reach stability. After its inoculation at day 0, *Bc* experienced growth and was able to establish in the community while displacing *Ca*, illustrating the classical scenario of a successful invasion. The top panel shows the time series of the pH measured at the end of each cycle. Vertical bars correspond to standard error of 3 technical replicates (often smaller than the curve width).

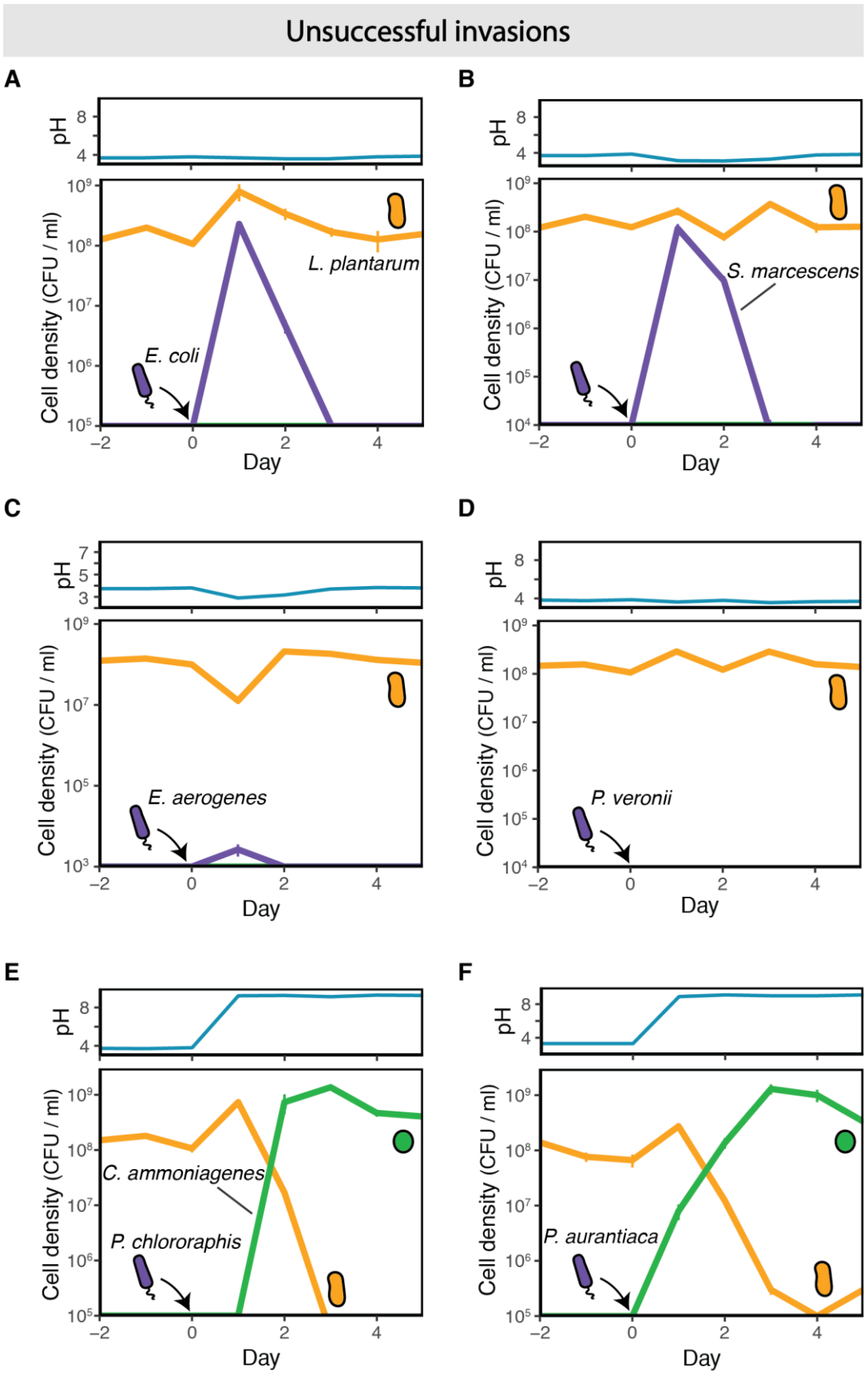
Unsuccessful invasions
A
B
C
D
E
F
pH
Cell density (CFU / ml)
Day
L. plantarum
E. coli
S. marcescens
E. aerogenes
P. veronii
C. ammoniagenes
P. chlororaphis
P. aurantiaca

Fig. S3. Six different species performed unsuccessful invasions into the *Ca* and *Lp* ecosystem. We initiated replicate cocultures at a 95:5 ratio of *Lp* to *Ca* cells, allowing 3 initial cycles for the system to reach stability. Selective plating on agar at the end of these initial cycles revealed no CFUs from *Ca*, indicating that *Ca* cells entering via migration were not able to survive an entire 24hr cycle in the stable state governed by *Lp*. **A**. After its inoculation at Day 0, *Ec* cells experienced growth and survived in the system during two cycles. However, *Ec* experienced extinction at day 3, indicating that this species had lost the competition with the resident community, which remained in the *Lp* stable state. **B-D.** Unsuccessful invasions by *Serratia marcescens (Sm)*, Enterobacter aerogenes (*Ea)*, and *Pv* species. Analogous to the case in A, these invasions mirrored classical unsuccessful invasions: the invader species experienced extinction without inducing significant change in the resident community. In D, *Pv* went extinct during the first 24hr cycle, as no CFU from this species were detected from agar plating at the end of the cycle. **E-F**. Unsuccessful invasions by *Pc* and *Pseudomonas aurantiaca (Pa)*, respectively, triggered switches from the *Lp* to the *Ca* stable state, but the invader species did not survive the transition. In panels E and F, agar plating at the end of each daily cycle did not allow us to detect the presence of the invader. Sampling the community with a higher frequency (fig. S4) revealed that the invader can grow to high densities during the first hours, nevertheless experiencing a rapid extinction once the high pH was reached, with no alive invader cells surviving until the next day. Panels E and F also show that the speed at which the transient invader induces the transition can change depending on the species. *Pa* invasions (panel F) favored the growth of *Ca* faster than *Pc* invasions (panel E). This is consistent with a potentially faster ability for *Pa* to modify the pH due to its faster growth in low (pH 5.5) and neutral (pH 6.5 and 7.5) pH conditions (Fig. 2E), although other factors intrinsic to each invader could also play a role. In all cases, time series for the cell population densities (main panels) and pH (top panels), both measured at the end of each cycle, are shown. Error bars (often smaller than the line width) in all panels show the standard error for 3 technical replicates. Data obtained from an independent experiment to the one in Fig. 1D.

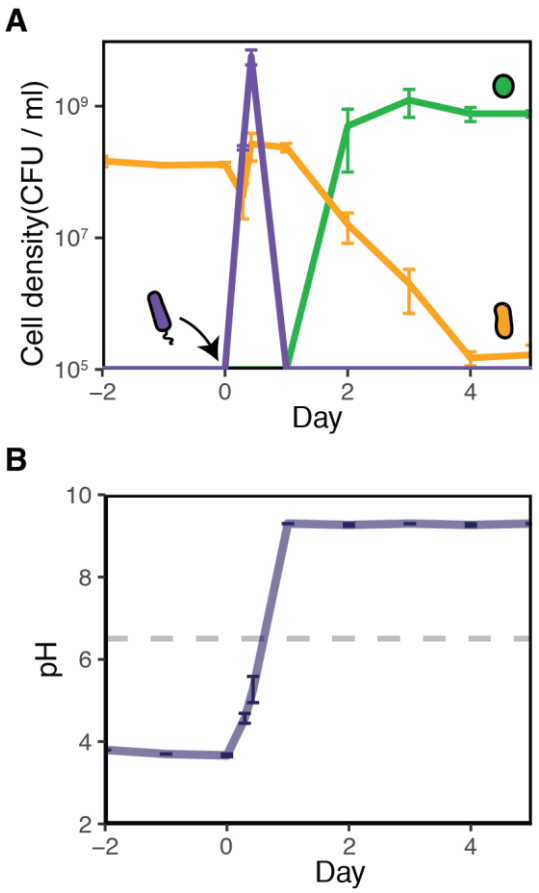

Fig. S4. The invader *Pc* thrives and decays within the 24 hours following inoculation into the *Lp* stable state. A. Time series for the cell density of *Lp* (orange), *Ca*(green) and *Pc* (purple) during a transient invasion that induced a switch between the two alternative states. Within the first 24hr after its inoculation, *Pc* grew to high density and experienced a following decay towards extinction. **B.** Time series for the observed pH revealing a rapid shift towards alkaline values following the inoculation of *Pc*. The rapid decay in the invader population in A occurs as the environment reaches high pH values that are unfavorable [44] for the invader. As a consequence, the number of invader cells that survive until day 1 (i.e. 24hr after the invader inoculation) is relatively low (Fig. 1D) or even below our detection limit (figs. S3E, S3F, and S4A). In order to avoid any potential contamination arising from the pH measurements at 7 and 10hr post-inoculation of *Pc*, we used additional replicate cocultures that were discarded after the measurements. Error bars indicate the standard error for 3 technical replicates from an independent experiment to those in Figs. 1D and S3.

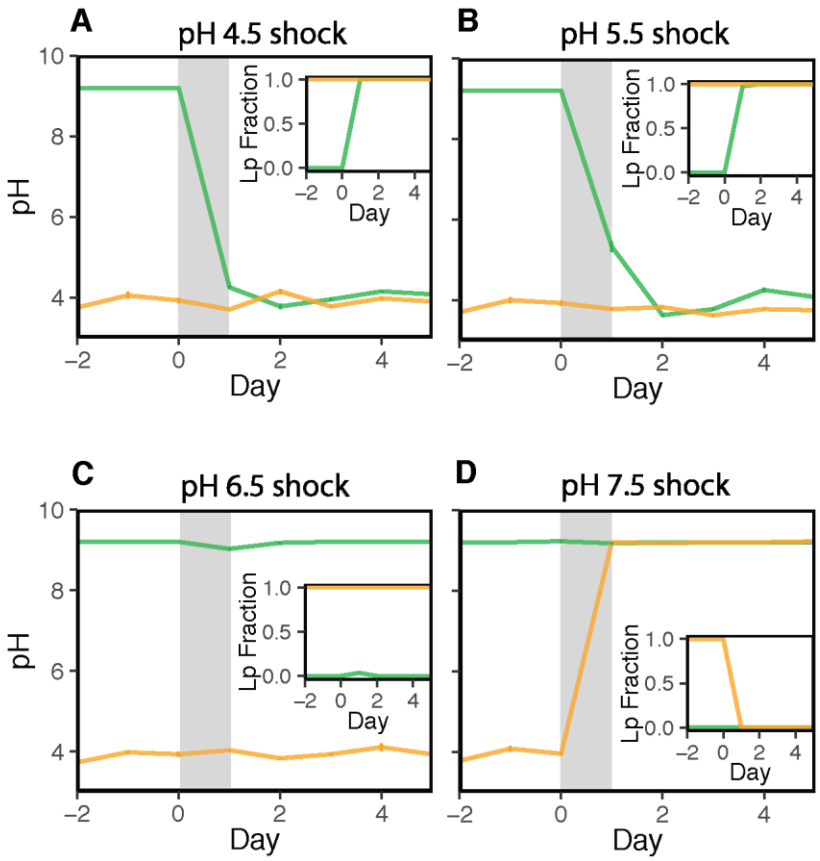

Fig. S5. Temporary perturbations in pH induce shifts between the *Lp* and *Ca* states. A. Starting at either 95:5 or 5:95 ratio of *Lp* to *Ca* cells, we allowed 3 cycles of dilution and migration for the system to reach the *Lp* stable state (orange) or the *Ca* stable state (green), respectively. At day 0, the cocultures were diluted into Supplemented Base Media buffered at pH 4.5 (100uM phosphate buffer) for only one cycle (shadowed area). This temporary shock induced a switch towards the *Lp* stable state in those cocultures that had previously reached the *Ca* stable state (green), while it did not significantly affect the cocultures that were already in the *Lp* state. **B.** Analogous to the previous case, a temporary shock at pH 5.5 triggered a switch from the *Ca* to the *Lp* stable state. **C.** A temporary shock at pH 6.5 did not significantly affect cocultures in either of the two stable states. **D.** A temporary shocks at pH 7.5 induced a switch from the *Lp* to the *Ca* stable state. In A-D, the main panel shows the time series for the pH measured at the end of each cycle, while the inset stands for the fraction of *Lp* cells in the system. Error bars (generally thinner than the line width) correspond to the standard error of 4 technical replicates.

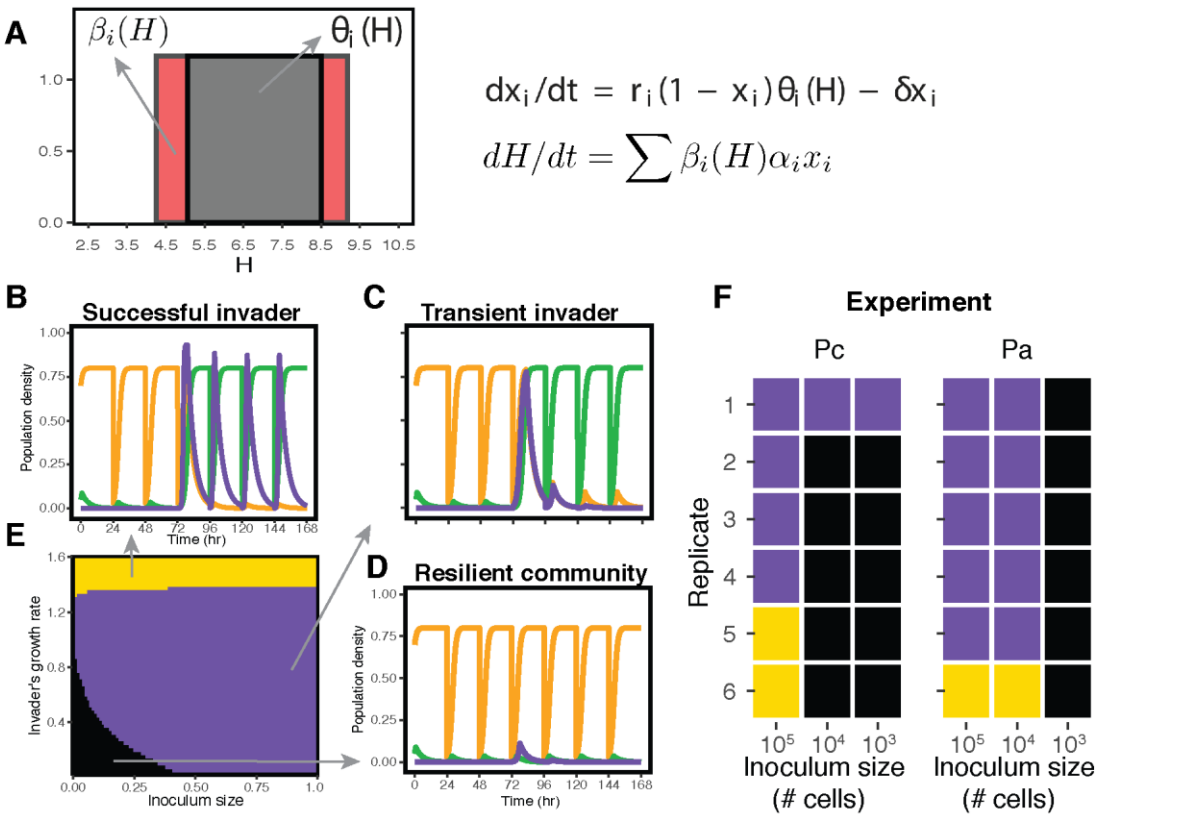

Fig. S6. Minimal model incorporating feedbacks between microbial growth and pH predicts a minimum inoculum size for the invasions to induce community shifts. A. The minimal model considers step functions that determine the range of pH tolerance (gray area) for each species, and the range in which microbes can modify the pH (red area). The density x_i of species *i* grows logistically (with maximum growth rate r_i) as long as the pH lies within its tolerance range θ_i. In addition, β_i determines the range in which each species can modify the pH at a rate α_i, as indicated by the set of equations. **B-D.** Time series for the species densities in three different scenarios, respectively: successful invasion in which the invader establishes, community shift induced by a transient invader, and resilience of the community against an unsuccessful invasion. **E.** The phase space for the three outcomes predicts a minimum inoculum size for transient invaders to induce a community shift, which lies at the interface between resilience (black region) and the shift between alternative stable states (purple). Parameter values for species 1: $r_1 = 1$, $\alpha_1 = -1$, $\theta_1 = [3.5,7.5]$, $\beta_1 = [3.8, 7.5]$. Parameter values for species 2: $r_2 = 1$, $\alpha_2 = 1$, $\theta_2 = [6,10]$, $\beta_2 = [6, 9.3]$. Parameter values for the invader species: $\alpha_3 = 1.1$, $\theta_3 = [5,8]$, $\beta_3 = [5, 8.5]$. **F.** Inoculating different initial amounts of invader cells showed that *Pc* and *Pa* require a minimum inoculum size to induce community shifts. In the experiment for the data in F, we observed some cases in which the invader had not reached extinction at the end of the experiment (2 out of 6 replicates when we inoculated 10^5 cells of *Pc*, 1 out of 6 replicates for two different inoculum sizes of *Pa* cells).

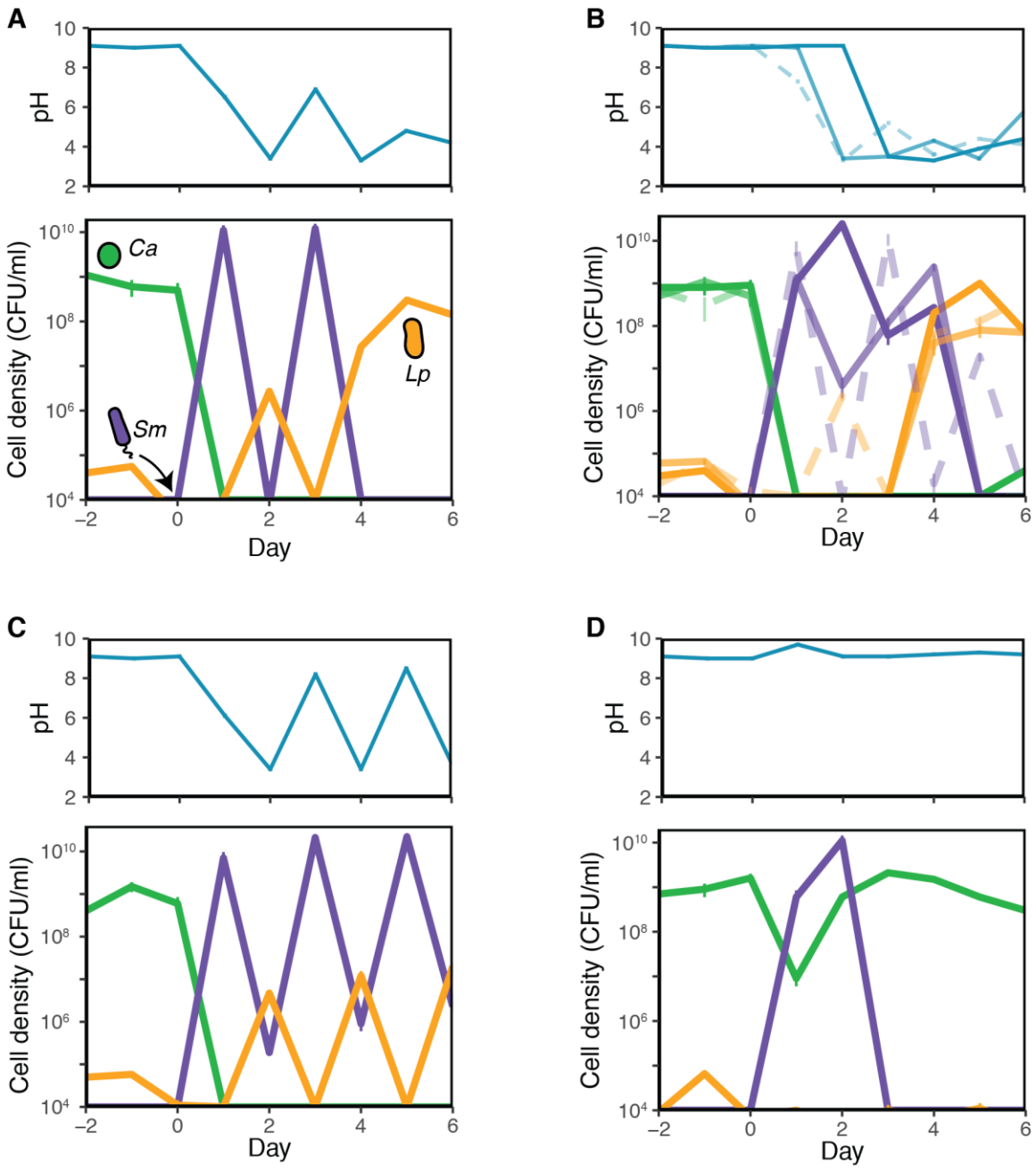

Fig. S7. The invader *Sm* can induce transitions from the alkaline (*Ca*) to the acidic (*Lp*) stable state. We observed a transition from the Ca to the Lp stable state in 4 out of 6 technical replicates, after inoculating *Sm* cells. **A.** Sm remained in the system for 3 cycles after its inoculation. The system reached the Lp stable state after *Sm* went extinct at Day 4. **B.** In these three replicates (solid, shade, and dashed lines) *Sm* was present in the system until Day 4 (5 in the case shown by the dashed line). No *Sm* cells were detected at the end of the experiment, and the system had transitioned into the *Lp* state. **C.** In one replicate *Sm* performed a successful invasion, as it coexisted with *Lp* until the end of the experiment. **D.** In this replicate *Sm* performed a (classical) unsuccessful invasion that did not induce a switch between stable states. In all the main panels, the error bars correspond to the standard deviation for a Poisson distribution centered at the observed CFU for each species in a single replicate. The upper panels correspond to the pH measurements for the cultures shown in the main panels.

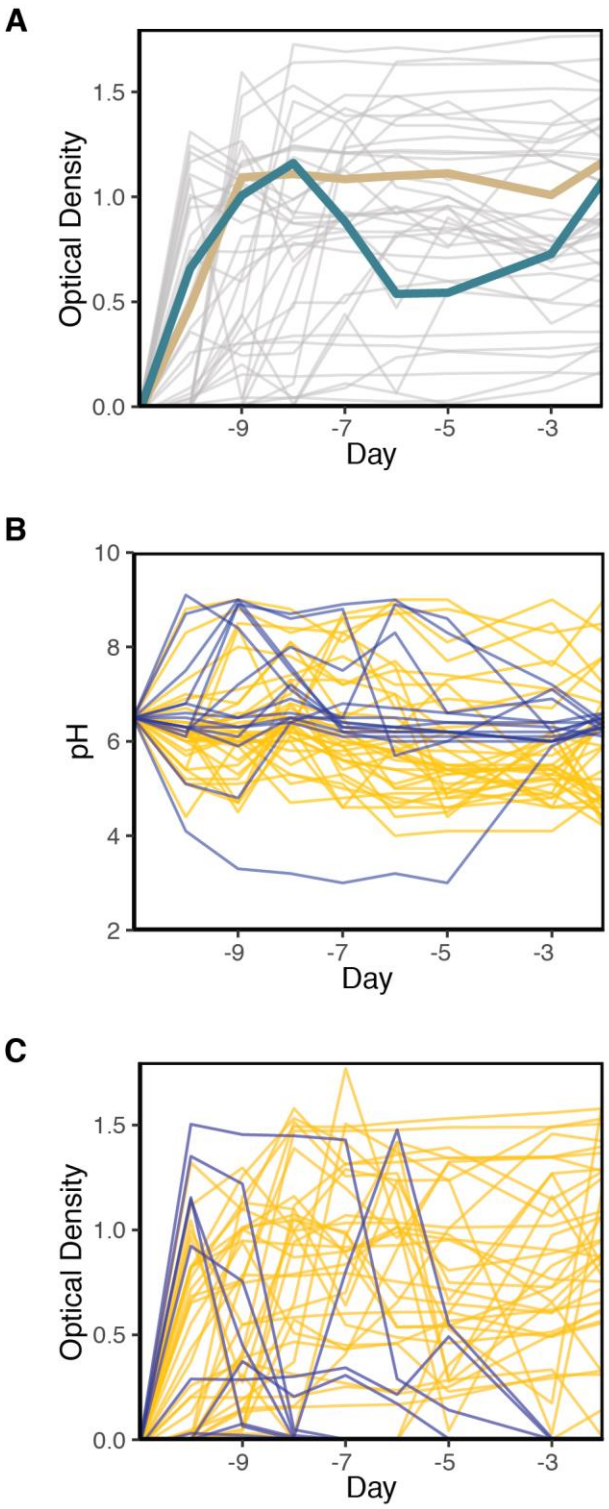

Fig. S8. Early dynamics of soil communities in laboratory environments. A. Time series for the optical density of the soil communities. The data corresponds to the 39 cultures shown in Fig. 3A, which exhibited signatures of pH stabilization (specifically, pH change between the last two cycles <0.5). **B.** pH time series for the additional 49 cultures that were inoculated with soil samples. Communities that went extinct during the experiment are shown in blue, and communities for which the pH was not stable (pH change between the last two cycles ≥0.5) are shown in yellow. **C.** Time series for the OD of the cultures shown in B.

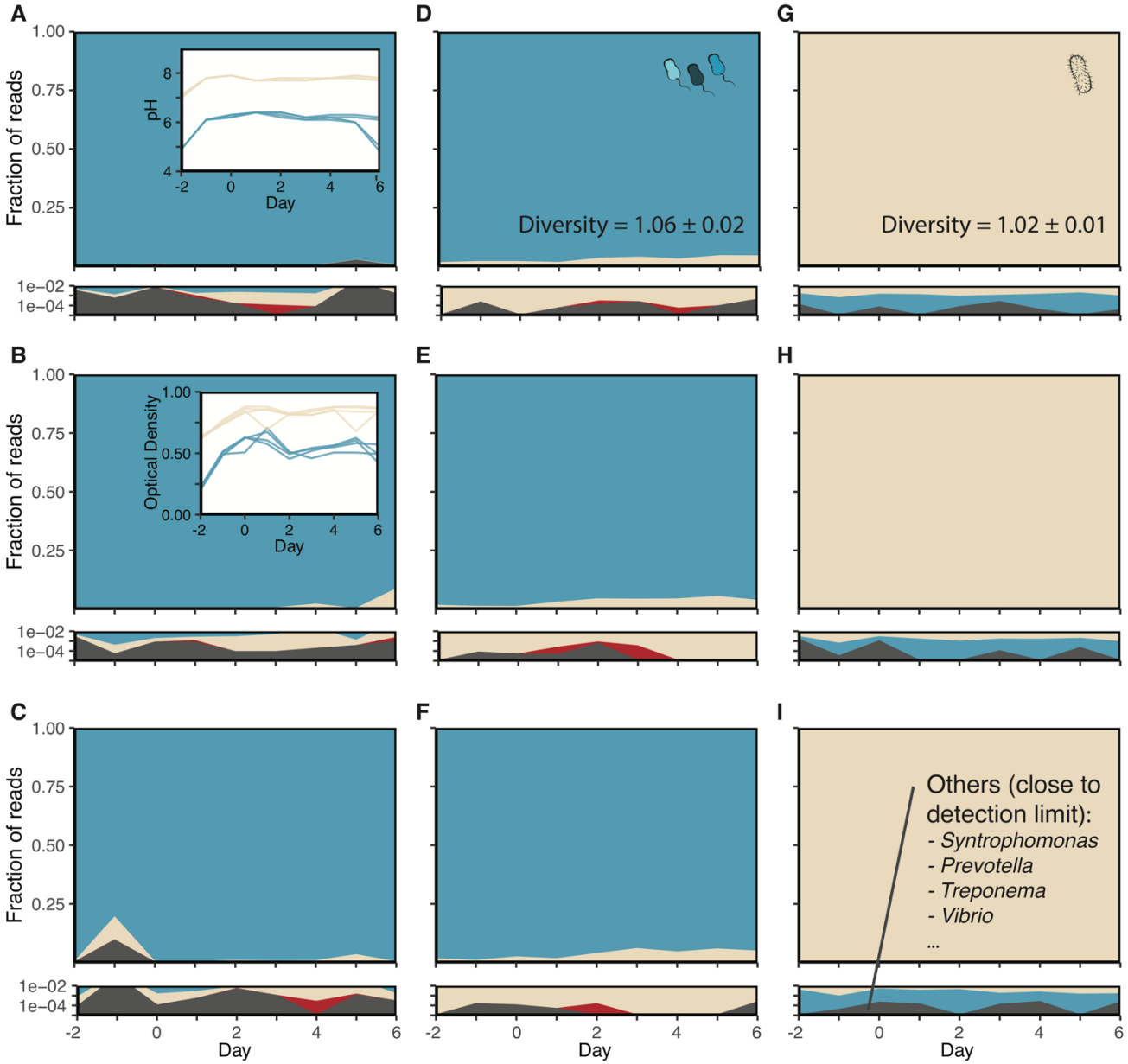

Fig. S9. Mutual resilience against migration between the *Bacillus* and *Pantoea* soil communities. A-C Time series for the fraction of 16S reads in 3 technical replicates in which the community dominated by Bacillus (blue) was exposed to migration by Pantoea (cream). Reads from *Pseudomonas* (red) and other (gray) sequence variants were occasionally detected at lower abundances (lower panels, shown in logarithmic scale). We sequenced 3 out of 4 technical replicates, for which pH and optical density measurements are shown in the insets of panels A and B, respectively, along with the same measurements for 4 replicates in which *Pantoea* was exposed to migration by *Bacillus* (lines in cream color in the insets of A and B). The data in A-C correspond to an independent experiment from the one in Fig. 3B. **D-I.** Fraction of 16S read abundances for cultures shown in Fig. 3B. In D-F, the community dominated by *Bacillus* was exposed to migration from *Pantoea*. In G-I, the community dominated by *Pantoea* was exposed to migration from *Bacillus*. We sequenced 3 out of the 4 replicates shown in Fig. 3B for each case. In all the replicate cultures we observed that the two communities were resilient to

migration from each other. D and G show the ^{1}D diversity number at Day 0 in the *Bacillus* and the *Pantoea* communities, respectively. The average and standard error of the effective diversity were computed for panels A-F and G-I, respectively. The low diversity in both communities indicate that each state is largely governed by just one ASV (the indicated ^{1}D diversity corresponds to $e^{H'}$, where H' is the Shannon-Wiener Index of the 16S reads). At very low fractions, often close to the detection limit, we found a turnover of other ASV corresponding to different species of *Bacillus*, *Pantoea* and *Pseudomonas*, in addition to *Syntrophomonas*, *Prevotella*, *Treponema*, among others. Occasionally, we also found rare reads associated to oceanic genus including *Vibrio* and *Reinekea*. We hypothesize that these rare reads correspond to low levels of cross-contamination during the DNA extraction, shipping and sequencing protocol, as some oceanic communities were also sent for sequencing in the same batch of samples.

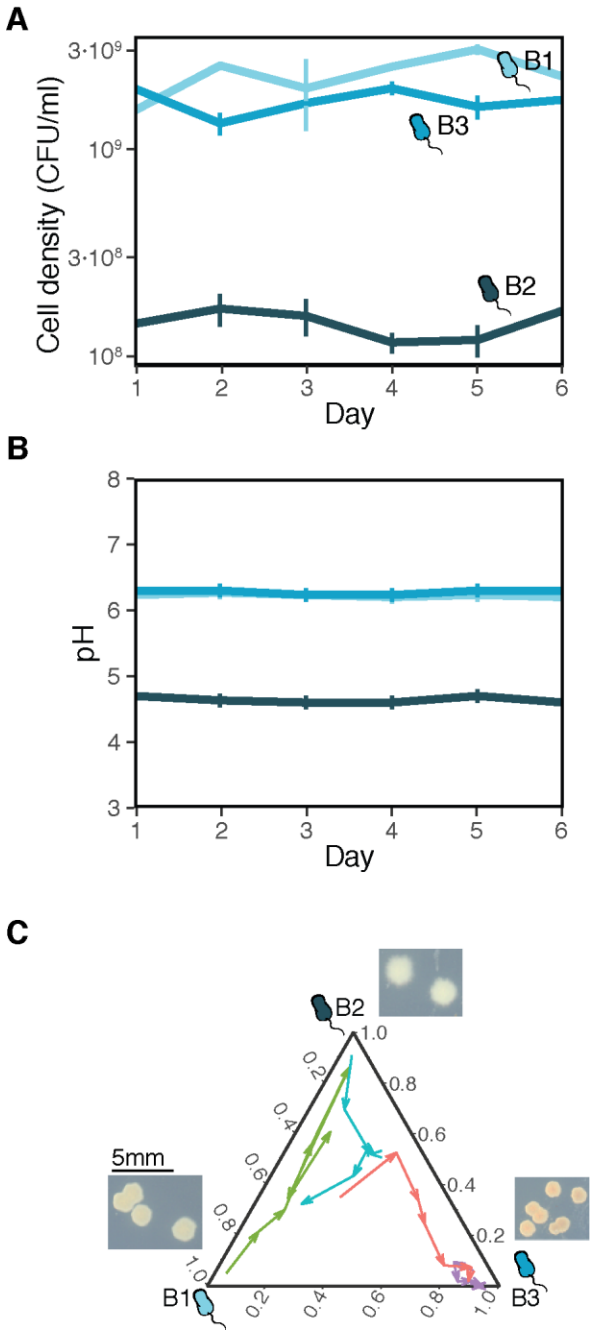

Fig. S10. Different behavior in laboratory microcosms for three genetically similar soil isolates. A. Time series for the cell density of monocultures from three strains isolated from the soil community (average and standard errors of 3 biological replicates exposed to the 30X daily dilution protocol described in the main text). Strain B2 exhibits a lower carrying capacity than strains B1 and B3. The three strains share the same 16S amplicon sequence, and were found in coexistence in one of the stable states described in Fig. 3. **B.** Time series for the pH (measured at the end of each cycle) of the monocultures in panel A. The strain B2 induces a more acidic pH than the one observed for the other two strains. **C.** Observed trajectories during a competition experiment in which the three isolates were mixed at different initial fractions (different arrow colors) and exposed to daily dilutions. The three edges of the simplex depict the abundance for the different strains. The observed trajectories indicate that the system can reach two alternative community compositions.

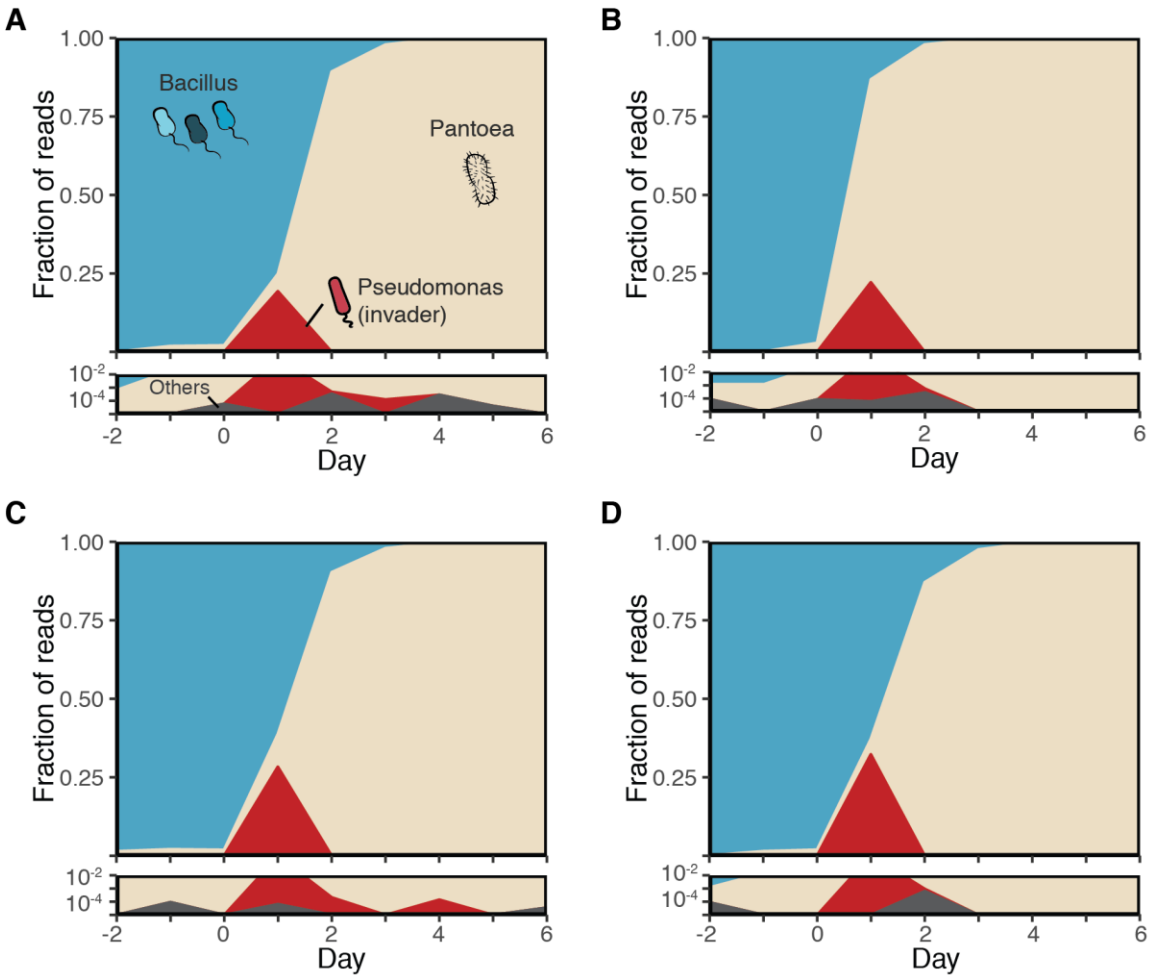

Fig. S11. Both *Pc* and *Pa* can induce transitions from the *Bacillus* to the *Pantoea* stable states. A-B Time series for the fraction of 16S reads showing the transition from the *Bacillus* stable state to the *Pantoea* stable state following inoculation of *Pc* (we sequenced two additional replicates of the invasion shown in Fig. 3C). In addition to the sequencing data (Fig. 3C, S11A and S11B), both the time series for the pH (Fig. 3D) and agar plating at the end of each daily cycle revealed analogous community dynamics in the 4 replicate invasions that we performed. **C-D** Time series for the fraction of 16S reads showing the transition from the *Bacillus* stable state to the *Pantoea* stable state, in this case following inoculation of *Pa* cells.